CLINICAL REPORT



# Electron Microscopic and Immunohistochemical Findings of the Epidermal Basement Membrane in Two Families with Nail-patella Syndrome

Satoru SHINKUMA[1,2]*, Hideki NAKAMURA[2], Manami MAEHARA[1], Shota TAKASHIMA[2], Toshifumi NOMURA[2], Yasuyuki FUJITA[2], Satoshi HASEGAWA[3], Kazuko C. SATO-MATSUMURA[4], Riichiro ABE[1] and Hiroshi SHIMIZU[2]

*[1]Division of Dermatology, Niigata University Graduate School of Medical and Dental Sciences, Niigata, [2]Department of Dermatology, Faculty of Medicine and Graduate School of Medicine, Hokkaido University, [3]Higashikariki Dermatology Clinic, and [4]Department of Dermatology, JCHO Sapporo Hokushin Hospital, Sapporo, Japan*

**Nail-patella syndrome is an autosomal dominant disorder characterized by nail dysplasia and skeletal anomaly. Some patients have been shown to have ultrastructural abnormalities of the glomerular basement membrane that result in nephrosis. However, little has been reported on the epidermal basement membrane in this condition. This paper reports 2 families with nail-patella syndrome. Direct sequencing analysis of *LMX1B* revealed that family 1 and family 2 were heterozygous for the mutations c.140-1G>C and c.326+1G>C, respectively. To evaluate the epidermal basement membrane zone, ultrastructural and immunohistochemical analyses were performed using skin specimens obtained from the dorsal thumb. Electron microscopy showed intact hemidesmosomes, lamina lucida, lamina densa, and anchoring fibrils. Immunofluorescence studies with antibodies against components of the epidermal basement membrane zone revealed a normal expression pattern among the components, including type IV collagen. These data suggest that nail dysplasia in patients with nail-patella syndrome is not caused by structural abnormalities of the epidermal basement membrane.**

*Key words:* epidermal basement membrane; glomerular basement membrane; hereditary osteo-onychodysplasia; LIM-homeodomain protein; LIM-homeobox transcription factor 1ß; LMX1B; type IV collagen.

Accepted Sep 12, 2019; E-published Sep 12, 2019

Acta Derm Venereol 2019; 99: 1110–1115.

*Corr:* Satoru Shinkuma, Division of Dermatology, Niigata University Graduate School of Medical and Dental Sciences, 1-757, Asahimachi-dori, Chuo-Ku, Niigata, 951-8510, Japan. *E-mail: shinkuma@med.niigata-u.ac.jp

## SIGNIFICANCE

Nail-patella syndrome is caused by mutations in the *LMX1B* gene that lead to anomalies of dorsal-ventral limb patterning. Some patients show abnormalities of the glomerular basement membranes; however, little is known about the epidermal basement membrane. This study found no abnormalities in the epidermal basement membrane zone. This finding suggests that nail deformities can be caused by the abnormal development of dorsal limb structures rather than dysfunction of the epidermal basement membrane.

Nail-patella syndrome (NPS; OMIM #161200) is characterized by nail dysplasia and skeletal anomalies, such as aplastic or hypoplastic patella, elbow abnormalities, and iliac horn (1). The disease is an autosomal dominant disorder caused by a heterozygous loss-of-function mutation in the *LMX1B* gene (OMIM #602575), encoding a member of the LIM homeobox transcription factor 1β, LMXIB (2). LMX1B functions as a transcription factor and is essential for the normal development of dorsal limb structures, the glomerular basement membrane (GBM), anterior segment of the eye, and dopaminergic and serotonergic neurones (3–7). Patients with NPS sometimes have nephrosis-associated renal disease (1). LMX1B regulates the expressions of type IV collagen (COL4) α3 and α4 (α3(IV) and α4(IV)) chains required for normal morphogenesis of GBM (4). Kidneys of some patients with NPS, therefore, show ultrastructural abnormalities including focal or diffuse irregular thickening of GBM with occasional regions of membrane discontinuity ("moth-eaten" appearance) (8, 9). However, little is known about the epidermal basement membrane (EBM). This study evaluated 2 families with NPS who were heterozygous for the splice-site mutations in *LMX1B*. We analysed the EBM in these families with NPS using electron microscopic and immunohistochemical techniques.

## MATERIALS AND METHODS

The medical ethics committee of Hokkaido University approved all the studies described herein. The study was conducted according to the principles of the Declaration of Helsinki. Written informed consent was obtained from the participants and/or their parents before the study procedures were conducted.

### *Patients*

Two families with NPS were enrolled in this study. Family 1 was referred to us with nail deformities since birth. The affected family members were a mother (I-2), 9-year-old boy (II-1), 7-year-old twin sisters (II-2 and II-3), and 7-month-old younger brother (II-4) (**Fig. 1**a). Their thumbnails exhibited dysplasia (Fig. 1b–e). They also had triangular lunulae on their index, middle and ring fingers. The creases of the skin overlying the distal interphalangeal joints of their fingers were missing (Fig. 1f).

doi: 10.2340/00015555-3318
Acta Derm Venereol 2019; 99: XX–XX

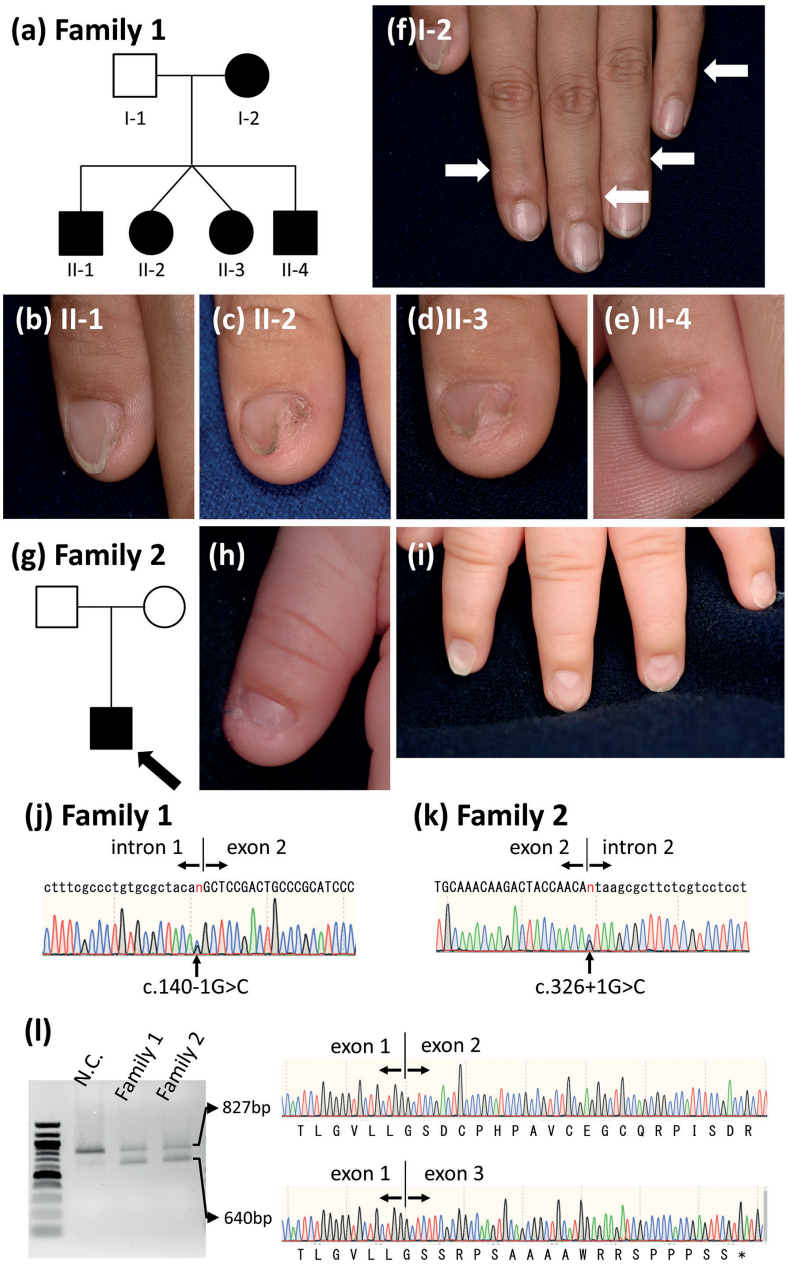


**Fig. 1. Clinical features and genetic analysis of family 1 and family 2.** (a) Pedigree of family 1. Affected individuals are indicated by *black shaded* shapes. (b–f) Clinical manifestations of family 1. Thumbnail dysplasia in the 4 children (b–e). The creases of the skin overlying the distal interphalangeal joints are missing (*arrow*) (f). (g) Pedigree of family 2. The proband is indicated by an arrow. (h, i) Clinical manifestations of thumbnails (h) and the other finger nails (i). (j, k) Affected family members of family 1 (j) and family 2 (k) are heterozygous for the splice-site mutations c.140-1G>C and c.326+1G>C, respectively. (l) Reverse transcriptase-PCR (RT-PCR) shows 2 splicing variants. The sequences of the RT-PCR products are subcloned using the TA cloning vector, and show a splice variant resulting in a frameshift and a subsequent premature termination codon (p.Asp49Serfs*17). N.C.: normal control.

In family 2, the proband was a 6-month-old boy. There was no family history of nail deformity (Fig. 1g). Clinically, he showed thumbnail dysplasia (Fig. 1h). Triangular lunulae and spoon nail were observed on his index, middle, ring, and little fingers. The creases of the skin overlying the distal interphalangeal joints of his fingers were missing (Fig. 1i).

*Genetic analysis*

*LMXIB* mutation search was performed as follows. Briefly, genomic DNA (gDNA) isolated from peripheral blood was subjected to PCR amplification, followed by direct automated sequencing using an ABI PRISM 3100 genetic analyser (Applied Biosystems, Framingham, MA, USA). Oligonucleotide primers were designed using a website program (http://www.bioinformatics.nl/cgi-bin/primer3plus/primer3plus.cgi). The entire coding regions of *LMXIB*, including the exon/intron boundaries, were sequenced using gDNA samples from patients and their family members. For normal controls, 50 healthy, ethnically matched individuals (100 normal alleles) were studied.

*RNA isolation and reverse transcription-PCR*

Total RNA was isolated from the dorsal thumb skin of the affected mother (I-2) of family 1 and the proband of family 2 using the RNeasy Mini Kit (QIAGEN, Hilden, Germany) and treated with DNase (Invitrogen, Carlsbad, CA, USA) to remove gDNA. Complementary DNA (cDNA) was synthesized using 3 μg RNA by the SuperScript IV reverse transcriptase (RT) (Invitrogen) and oligo-dT primer (Invitrogen) according to the manufacturer's instructions. Using the first-strand cDNA as a template, the LMX1B cDNA was amplified using primers that were designed in exon 1 (5'-ATAGCAACAGGTCCCGAGTC-3') and exons 5–6 (5'-GCCAGCTTCTTCATCTTTGC-3') of the LMX1B cDNA. The PCR products were TA-cloned into the pCRII-TOPO vector (Invitrogen), and then each clone was sequenced separately.

*Electron microscopy*

Skin biopsy samples were fixed with a 5% glutaraldehyde in 0.1M cacodylate buffer, followed by post-fixation with 1% osmium tetroxide in 0.1M cacodylate buffer. After dehydration steps in a graded ethanol series, the samples were embedded in TAAB EPON 812 resin (TAAB, Aldermaston, UK). Ultrathin sections (60–70 nm) were stained with uranyl acetate and lead citrate (10) and examined by JEM1400 transmission electron microscopy (JEOL Ltd, Akishima, Tokyo, Japan) at 80 kV.

*Immunofluorescence analysis*

Immunofluorescence analysis was performed using skin specimens obtained from the dorsal thumb of the affected mother (I-2) of family 1 and the proband of family 2. Fresh skin specimens were embedded in an optimal cutting temperature compound (Sakura Finetek, Torrance, CA, USA) and quickly frozen with dry ice. Five-μm cryostat sections were incubated with primary antibodies overnight at 4°C. After washing in phosphate-buffered saline, the sections were incubated with secondary antibodies conjugated with fluorescein-isothiocyanate (FITC) for 1 h at room temperature. All the stained samples were observed using a confocal laser scanning microscope (Fluoview FV1000, Olympus Optical Co. Ltd, Tokyo, Japan).

*Antibodies*

The following antibodies against basement membrane zone components were used: monoclonal antibodies (mAbs) GoH3 and 3E1 (Chemicon International, Temecula, CA, USA) against α6 and β4 integrin subunits, respectively; mAb GB3 (Sera-lab, Sussex, UK) against laminin 332 (laminin γ2 chain) (11); mAb LH 7.2 (Sigma-Aldrich, St Louis, MO, USA) against type VII collagen; polyclonal Ab S1193 against dystonin (BPAG1); C17-C1 against type XVII collagen (12); and HD1-121 against plectin. S1193 and HD1-121 were generously donated by Professor J. R. Stanley of the University of Pennsylvania, USA and Professor Owaribe of Nagoya University, Japan, respectively. For COL4, PHM-12+CIV22 (Thermo Fisher Scientific, Rockford, IL, USA), Texas Red-conjugated H25 (Shigei Medical Research Institute, Okayama, Japan), FITC-conjugated H53+B51 (Shigei Medical Research Institute), H31 (Chondrex, Redmond, WA, USA), and H43 (Chondrex) were used.

*Normal ultrastructural appearance of the epidermal basement membrane zone*

Samples were obtained from the dorsal thumb skin of the affected mother (I-2) of family 1 and the proband of family 2 because the thumbnail deformity was the most prominent. Electron microscopy revealed no remarkable thickening and redundancy of the EBM, which were previously detected in a nail-patella syndrome patient (13). Tonofilament accumulation in the basal cells and disrupted and discontinuous lamina densa, which were detected in the gingiva or skin of Alport syndrome, were not observed in our patient skin (14, 15). The other complicated structures including the lamina lucida, hemidesmosomes, and anchoring fibrils, were intact (**Fig. 2**a, b).

## RESULTS

*Detection of novel splice-site mutations in* LMX1B

Direct sequencing analysis of exons and intron-exon boundaries of *LMX1B* revealed that family 1 and family 2 were heterozygous for the mutations c.140-1G>C and c.326+1G>C, respectively (RefSeq: NM_001174146.1) (Fig. 1j, k). Moreover, we confirmed that the splice-site mutations were absent in the healthy family members, as well as in the 50 ethnically matched control individuals and Exome Aggregation Consortium (exac.broadinstitute.org/).

*Exon skipping with frameshift resulting from splice-site mutations*

Since c.140-1G>C and c.326+1G>C were located at the exon-intron boundaries, we performed splice variant analysis using RT-PCR of cDNA extracted from the dorsal thumb skin of the affected mother (I-2) of family 1 and the proband of family 2. The cDNA was amplified using primers designated in exon 1 and exons 5–6, which showed 2 transcripts, 827 bp (transcript 1) and 640 bp (transcript 2), in family 1 and family 2 (Fig. 1l). Cloning and direct sequencing of the amplified fragments revealed that transcript 1 was wild-type. In transcript 2, exon 2 was skipped and exon 1 was directly connected to exon 3, resulting in a frameshift and a subsequent premature termination codon (p.Asp49Serfs*17) (Fig. 1l).

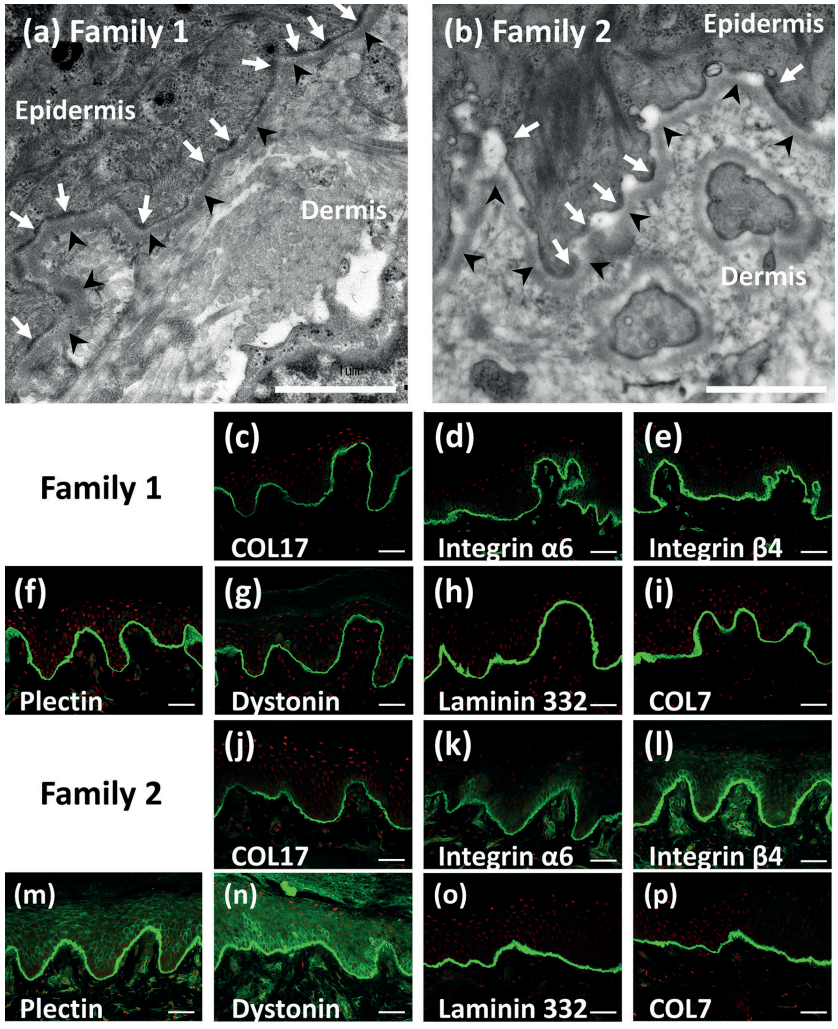


**Fig. 2. Electron microscopic findings and immunofluorescence mapping with antibodies to components of the epidermal basement membrane zone.** Electron microscopic findings of the skin obtained from (a) the dorsal thumb of I-2 in family 1, and (b) the proband of family 2, reveal no irregular thickening of the basement membrane as is observed in the glomerula of patients with nail-patella syndrome. *White arrows* and *black arrowheads* indicate hemidesmosomes and lamina densa, respectively. Scale bars=1 μm. Immunostaining for type XVII collagen (COL17), α6 and β4 integrin subunits, plectin, dystonin, laminin 332, and type VII collagen (COL7) (green) reveal normal dermo-epidermal junction labelling patterns in (c–i) family 1 and (j–p) family 2. Red represents propidium iodide. *Scale bars*=50 μm.

*Protein expression patterns of the epidermal basement membrane zone*

Extensive immunofluorescence analysis of the skin specimens from the dorsal thumb of the affected mother (I-2) of family 1 and the proband of family 2 was performed using several antibodies that react with molecules of the dermo-epidermal junction (DEJ). Immunostaining for α6 and β4 integrin subunits, laminin 332, type VII collagen, dystonin, type XVII collagen, and plectin revealed normal DEJ labelling patterns (Fig. 2c–p).

We used 5 antibodies: PHM-12+CIV22 (α1(IV) and/or α2(IV) (epitopes were not determined)), H25 (α2(IV)), H31 (α3(IV)), H43 (α4(IV)), and H53+B51 (α5(IV)), respectively, to assess COL4 expression patterns in the skin specimens. As previously reported (16), EBM contained the $[\alpha1(IV)]_2/\alpha2(IV)$ and $[\alpha5(IV)]_2/\alpha6(IV)$ molecules, but not the α3(IV)/α4(IV)/α5(IV) molecules. There was no difference between the patients with NPS and healthy human controls in the expression levels of COL4 subunits (**Fig. 3**).

## DISCUSSION

The EBM is a complex assembly of proteins that play a key role in dermal–epidermal adhesion and regulates many important processes, such as development and wound healing. COL4 is a main structural component of basement membranes and there are 6 different α chains: α1(IV) – α6 (IV) (17). COL4 forms 3 types of triple-helical heterotrimers consisting of the 2 α1(IV)

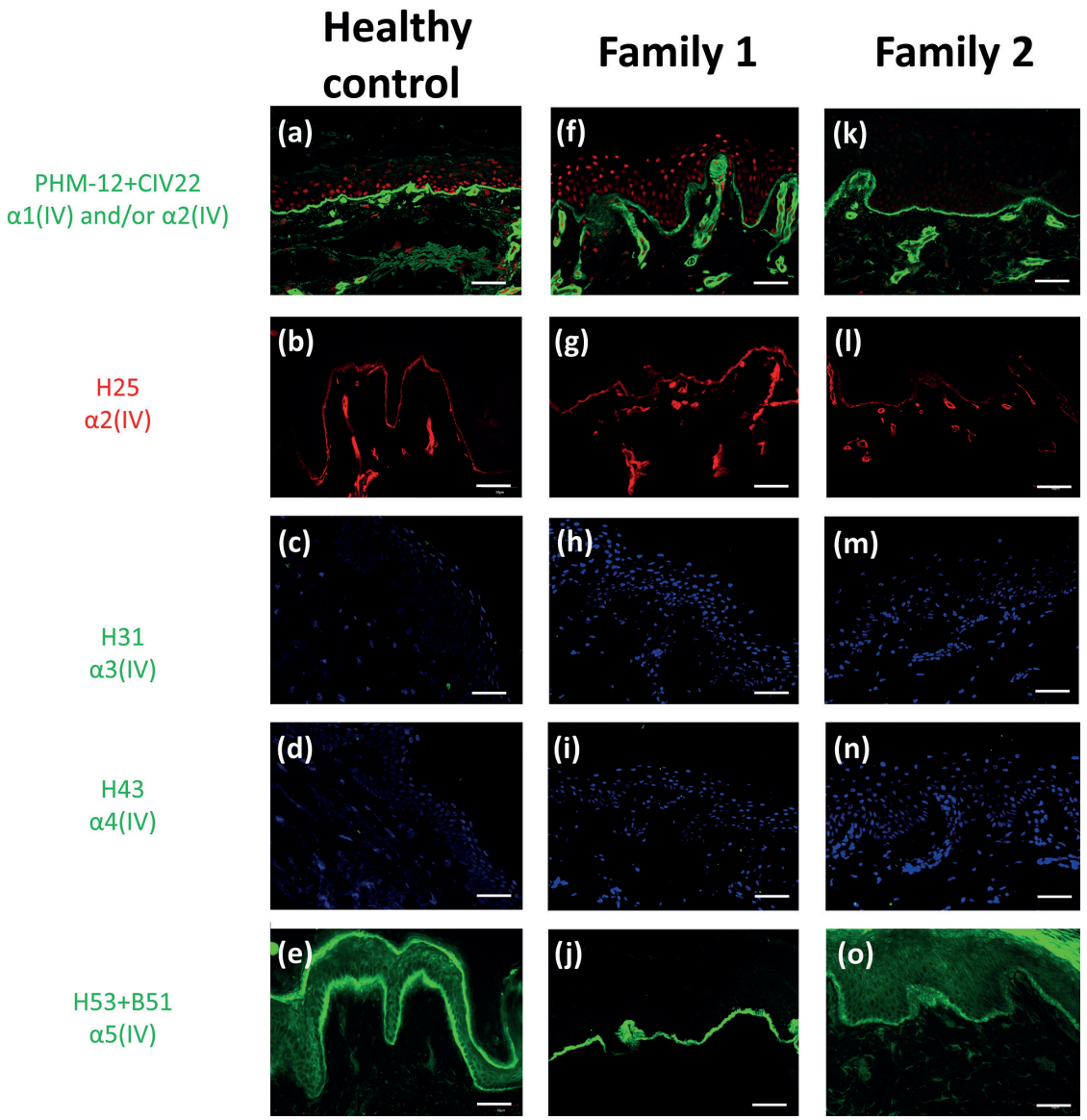


**Fig. 3. Type IV collagen expression patterns of the epidermal basement membrane zone.** Five antibodies: PHM-12+CIV22 (α1(IV) and/or α2(IV) (epitopes are not determined)), H25 (α2(IV)), H31 (α3(IV)), H43 (α4(IV)), and H53+B51 (α5(IV)), are used to evaluate type IV collagen expression patterns in the skin specimens. Expression levels of (f–j) family 1 and (k–o) family 2 are almost the same as those of (a–e) the healthy control. *Red* in a, f, and k represents propidium iodide. *Blue* in c, d, h, i, m, and n represents 4',6-diamidino-2-phenylindole. *Scale bars*=50 μm.

and 1 α2(IV) chains; 1 α3(IV), 1 α4(IV) and 1 α5(IV) chains; and 2 α5(IV) and 1 α6(IV) chains (18). Two heterotrimeric molecules are detected in GBM of mature mammals; the [α1(IV)]2/α2(IV) and α3(IV)/α4(IV)/α5(IV) molecules are distributed in the sub-endothelial and sub-epithelial layers of GBM, respectively (19, 20). Congenital anomalies of the α3(IV)/α4(IV)/α5(IV) molecules are associated with defects in molecular filtration resulting in Alport syndrome (21). Some patients with NPS have renal diseases, such as nephropathy characterized by ultrastructural abnormalities of GBM (2, 9). *Lmx1b* knockout mice have strongly decreased expressions of the α3(IV) and α4(IV) chains in GBM (4). In addition, LMX1B binds to a putative enhancer sequence in intron 1 of both mouse and human *COL4A4* and upregulates reporter constructs containing this enhancer-like sequence (4). These data indicate that LMX1B regulates the expressions of α3(IV) and α4(IV), the main components of the sub-epithelial layers of GBM, and that its dysregulation leads to the morphological abnormalities of GBM and nephrosis in NPS (4).

The EBM zone is composed of various complexes (22). Hemidesmosomes consist of plectin, dystonin, α6β4 integrin and type XVII collagen. Lamina densa and anchoring fibrils comprise COL4 and type VII collagen, respectively. Each of the components plays a crucial role in DEJ adhesion and regulates development and wound healing (23). Two heterotrimeric COL4 molecules, $[\alpha1(IV)]_2/\alpha2(IV)$ and $[\alpha5(IV)]_2/\alpha6(IV)$, are detected in the EBM zone (16). Since abnormalities of the EBM zone lead to nail deformities which are also observed in patients with dystrophic epidermolysis bullosa (24), we evaluated EBM in patients with NPS. Electron microscopy showed intact hemidesmosomes, lamina lucida, lamina densa, and anchoring fibrils. Immunofluorescence studies with antibodies against components of the EBM zone revealed normal expression patterns among them. Moreover, in order to analyse COL4 in more detail, we performed an immunofluorescence study using several COL4 monoclonal antibodies against α1(IV) and/or α2(IV), α2(IV), α3(IV), α4(IV), and α5(IV), and the results revealed that there was no distinct difference between patients with NPS and healthy controls. LMX1B plays a crucial role in the determination of dorsal-ventral limb patterning in the developing limb (3, 25). *LMX1B* mutant mice showed loss of dorsal features, such as the absence of the patella, and duplication of the ventral muscle and tendon pattern in the dorsal limbs at the level of the metatarsals (26). In the forelimbs, dorsal features (hair follicles) were missing and replaced by ventral features (foot pads), and the nails appeared to be missing. Taken together, nail deformities in patients with NPS are caused by the abnormal development of dorsal limb structures, rather than dysfunction of the EBM (**Fig. 4**).

Genetic analysis of NPS has so far determined that haploinsufficiency of LMX1B leads to the clinical manifestation of NPS (27). In this study, we evaluated 2 families with NPS. Direct sequencing analysis revealed that family 1 and family 2 were heterozygous for the splice-site mutations, c.140-1G>C (IVS1-1G>C) and c.326+1G>C (IVS2+1G>C) in *LMX1B*, respectively. To identify the mechanism of pathogenesis, we performed RT-PCR of cDNA extracted from the dorsal skins of their thumbs, which showed normal and shortened PCR products in both samples. Intriguingly, sequencing of the shortened PCR products revealed the same splice variant with deletion of exon 2, leading to a frameshift and a downstream premature termination codon (p.Asp49Serfs*17). Our data confirm that NPS is caused by haploinsufficiency of LMX1B as previously reported (27).

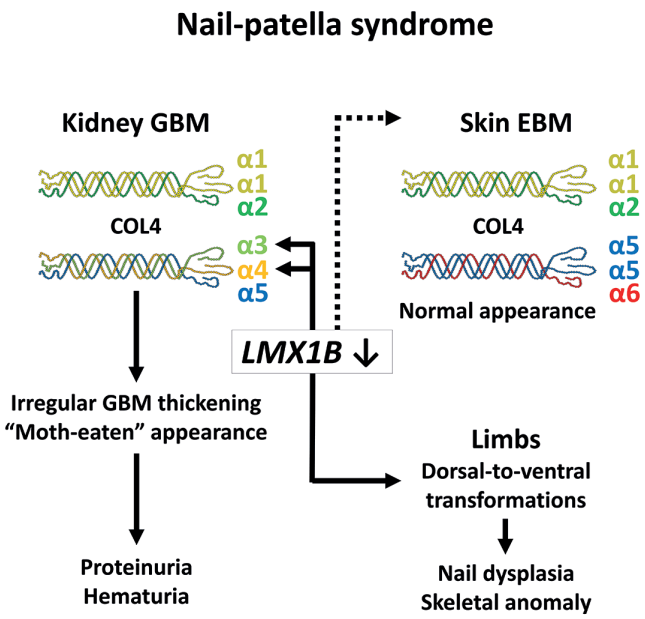


**Fig. 4. Schematic diagram of the potential pathogenesis of nail-patella syndrome.** Nail-patella syndrome is an autosomal dominant disorder caused by a mutation in the *LMX1B* gene, encoding LMXIB. LMX1B, which functions as a transcription factor, is essential for the normal development of dorsal limb structures and the renal glomerular basement membrane (GBM). LMX1B regulates the expressions of type IV collagen (COL4) α3 and α4, the main components of the subepithelial layers of GBM, and its dysregulation leads to the morphological abnormalities of GBM and nephrosis. However, epidermal basement membrane (EBM) are intact in our patients with nail-patella syndrome because α3 and α4 subunits of COL4 are not expressed in the skin.

In conclusion, we describe here 2 families with NPS, both heterozygous for the distinct splice-site mutations in *LMX1B*, resulting in skipping of exon 2. Electron microscopy and immunohistochemistry were used to analyse the EBM zone: no significant differences in EBM were found between patients with NPS and the healthy control group. This study suggests that nail dysplasia in NPS patients is not caused by abnormalities of the EBM.

## ACKNOWLEDGEMENTS

The authors are most grateful to the patients and their family members for their participation in this study. This work was supported

by a Grant-in-Aid for Young Scientists (A) 17H05089 (to S.S.) and Grant-in-Aid for Scientific Research (A) 17H01572 (to H.S.) from the Japan Society for the Promotion of Science Japan and Japanese Dermatological Association for the Basic Dermatological Research from Shiseido.

## REFERENCES

1. Sweeney E, Fryer A, Mountford R, Green A, McIntosh I. Nail patella syndrome: a review of the phenotype aided by developmental biology. J Med Genet 2003; 40: 153–162.
2. Dreyer SD, Zhou G, Baldini A, Winterpacht A, Zabel B, Cole W, et al. Mutations in LMX1B cause abnormal skeletal patterning and renal dysplasia in nail patella syndrome. Nat Genet 1998; 19: 47–50.
3. Riddle RD, Ensini M, Nelson C, Tsuchida T, Jessell TM, Tabin C. Induction of the LIM homeobox gene Lmx1 by WNT7a establishes dorsoventral pattern in the vertebrate limb. Cell 1995; 83: 631–640.
4. Morello R, Zhou G, Dreyer SD, Harvey SJ, Ninomiya Y, Thorner PS, et al. Regulation of glomerular basement membrane collagen expression by LMX1B contributes to renal disease in nail patella syndrome. Nat Genet 2001; 27: 205–208.
5. Pressman CL, Chen H, Johnson RL. LMX1B, a LIM homeodomain class transcription factor, is necessary for normal development of multiple tissues in the anterior segment of the murine eye. Genesis 2000; 26: 15–25.
6. Smidt MP, Asbreuk CH, Cox JJ, Chen H, Johnson RL, Burbach JP. A second independent pathway for development of mesencephalic dopaminergic neurons requires Lmx1b. Nat Neurosci 2000; 3: 337–341.
7. Ding YQ, Marklund U, Yuan W, Yin J, Wegman L, Ericson J, et al. Lmx1b is essential for the development of serotonergic neurons. Nat Neurosci 2003; 6: 933–938.
8. Heidet L, Bongers EM, Sich M, Zhang SY, Loirat C, Meyrier A, et al. In vivo expression of putative LMX1B targets in nail-patella syndrome kidneys. Am J Pathol 2003; 163: 145–155.
9. Taguchi T, Takebayashi S, Nishimura M, Tsuru N. Nephropathy of nail-patella syndrome. Ultrastruct Pathol 1988; 12: 175–183.
10. Richardson KC, Jarett L, Finke EH. Embedding in epoxy resins for ultrathin sectioning in electron microscopy. Stain Technol 1960; 35: 313–323.
11. Matsui C, Nelson CF, Hernandez GT, Herron GS, Bauer EA, Hoeffler WK. Gamma 2 chain of laminin-5 is recognized by monoclonal antibody GB3. J Invest Dermatol 1995; 105: 648–652.
12. Wada M, Nishie W, Ujiie H, Izumi K, Iwata H, Natsuga K, et al. Epitope-dependent pathogenicity of antibodies targeting a major bullous pemphigoid autoantigen collagen XVII/BP180. J Invest Dermatol 2016; 136: 938–946.
13. Burkhart CG, Bhumbra R, Iannone AM. Nail-patella syndrome. A distinctive clinical and electron microscopic presentation. J Am Acad Dermatol 1980; 3: 251–256.
14. Kuroki A, Ito J, Yokochi A, Kato N, Sugisaki T, Sueki H, et al. Diagnosing Alport syndrome using electron microscopy of the skin. Kidney Int 2008; 73: 364–365.
15. Toygar HU, Toygar O, Guzeldemir E, Cilasun U, Nacar A, Bal N. Alport syndrome: significance of gingival biopsy in the initial diagnosis and periodontal evaluation after renal transplantation. J Appl Oral Sci 2009; 17: 623–629.
16. Hasegawa H, Naito I, Nakano K, Momota R, Nishida K, Taguchi T, et al. The distributions of type IV collagen alpha chains in basement membranes of human epidermis and skin appendages. Arch Histol Cytol 2007; 70: 255–265.
17. Sado Y, Kagawa M, Naito I, Ueki Y, Seki T, Momota R, et al. Organization and expression of basement membrane collagen IV genes and their roles in human disorders. J Biochem 1998; 123: 767–776.
18. Khoshnoodi J, Pedchenko V, Hudson BG. Mammalian collagen IV. Microsc Res Tech 2008; 71: 357–370.
19. Gunwar S, Ballester F, Noelken ME, Sado Y, Ninomiya Y, Hudson BG. Glomerular basement membrane. Identification of a novel disulfide-cross-linked network of alpha3, alpha4, and alpha5 chains of type IV collagen and its implications for the pathogenesis of Alport syndrome. J Biol Chem 1998; 273: 8767–8775.
20. Sado Y, Kagawa M, Kishiro Y, Sugihara K, Naito I, Seyer JM, et al. Establishment by the rat lymph node method of epitope-defined monoclonal antibodies recognizing the six different alpha chains of human type IV collagen. Histochem Cell Biol 1995; 104: 267–275.
21. Cosgrove D, Liu S. Collagen IV diseases: a focus on the glomerular basement membrane in Alport syndrome. Matrix Biol 2017; 57–58: 45–54.
22. Shinkuma S, McMillan JR, Shimizu H. Ultrastructure and molecular pathogenesis of epidermolysis bullosa. Clin Dermatol 2011; 29: 412–419.
23. Tsuruta D, Hashimoto T, Hamill KJ, Jones JC. Hemidesmosomes and focal contact proteins: functions and cross-talk in keratinocytes, bullous diseases and wound healing. J Dermatol Sci 2011; 62: 1–7.
24. Shinkuma S. Dystrophic epidermolysis bullosa: a review. Clin Cosmet Investig Dermatol 2015; 8: 275–284.
25. Vogel A, Rodriguez C, Warnken W, Izpisua Belmonte JC. Dorsal cell fate specified by chick Lmx1 during vertebrate limb development. Nature 1995; 378: 716–720.
26. Chen H, Lun Y, Ovchinnikov D, Kokubo H, Oberg KC, Pepicelli CV, et al. Limb and kidney defects in Lmx1b mutant mice suggest an involvement of LMX1B in human nail patella syndrome. Nat Genet 1998; 19: 51–55.
27. Mukai M, Fujita H, Umegaki-Arao N, Sasaki T, Yasuda-Sekiguchi F, Isojima T, et al. A familial case of nail patella syndrome with a heterozygous in-frame indel mutation in the LIM domain of LMX1B. J Dermatol Sci 2018; 90: 90–93.